



Published in final edited form as:

*Anal Chem.* 2012 August 7; 84(15): 6317–6320. doi:10.1021/ac301541r.

## Separation of Variant Methylated Histone Tails by Differential Ion Mobility

Alexandre A. Shvartsburg<sup>\*</sup>, Yupeng Zheng<sup>†</sup>, Richard D. Smith<sup>\*</sup>, and Neil L. Kelleher<sup>†</sup>

<sup>\*</sup>Biological Sciences Division, Pacific Northwest National Laboratory, Richland, WA 99352

<sup>†</sup>Department of Chemistry, Department of Molecular Biosciences, and the Chemistry of Life Processes Institute, Northwestern University, Evanston, IL 60208

### Abstract

Differential ion mobility spectrometry (FAIMS) is emerging as a broadly useful tool for separation of isomeric modified peptides with post-translational modifications (PTMs) attached to alternative residues. Such separations were anticipated to become more challenging for smaller PTMs and longer peptides. Here we show that FAIMS can fully resolve localization variants involving a PTM as minuscule as methylation, even for larger peptides in the middle-down range.

### Introduction

Biological activity of proteins is largely controlled by post-translational modifications (PTMs). A stellar example is histones and specifically their N-terminal tails, where rich interdependent patterns involving diverse PTMs appear to make up an epigenetic code.<sup>1,2</sup> Hence characterization and quantification of PTMs is essential to proteomics.<sup>3</sup> Much effort has focused on discovering new PTMs and enriching for and detecting the presence of frequent PTMs such as phosphorylation, glycosylation, nitration, acetylation, and methylation. Pinpointing the position of a PTM on the backbone is also critical, as even minimal shifts can dramatically change the protein function.<sup>2,4</sup> For instance, dimethylation of H3 histone is associated<sup>2</sup> with transcription activation when on the K4 residue but with heterochromatin and repression when on the neighboring lysine (K9).

Localizing PTMs normally involves tandem mass spectrometry (MS/MS) of either an intact protein or proteolytic peptides via collision-induced dissociation (CID) or electron capture or transfer dissociation (EC/TD).<sup>5</sup> Unlike CID, EC/TD mostly avoids cleaving weak bonds to PTMs, moving PTMs between sites, or causing other potentially misleading isomerizations.<sup>6</sup> Still, EC/TD has limited sensitivity because of low overall efficiency and distribution of ion signal into many fragment channels,<sup>7</sup> and works poorly or not at all for peptides with the charge state ( $z$ ) of 1 or 2 or “electron predator” PTMs such as nitrate.<sup>8</sup> As all MS/MS methods, EC/TD is challenged by sequences where alternative PTM sites are proximal, which yield just one or few distinguishing fragments. A major problem is that multiple PTM localization variants of proteins ubiquitously coexist, commonly with dissimilar populations. Many of these translate into variant peptides upon digestion, especially with non-tryptic proteases that yield longer sequences and therefore higher  $z$  preferred for EC/TD. Mixtures of three or more of such species cannot be disentangled by MS/MS in principle, because of non-unique product masses for all parents except two.<sup>9</sup> While proteolytic digests are usually fractionated by liquid chromatography (LC) prior to MS/MS, LC often fails to separate localization variants, especially those with nearby alternatively occupied sites.<sup>10</sup> In particular, histones with different number of acetylations or methylations are separable by hydrophilic interaction LC (HILIC), but variants for each number generally co-elute.<sup>11,12</sup>

Localization variants of modified peptides were recently resolved by ion mobility spectrometry (IMS), both conventional IMS<sup>13</sup> measuring the absolute mobility ( $K$ ) at moderate electric field strength ( $E$ ) and differential or field asymmetric waveform IMS (FAIMS)<sup>9,14–16</sup> based on the difference between  $K$  values at high and low  $E$ . In FAIMS, species with a certain derivative of  $K(E)$  over a range of  $E$  are selected while traversing a gap between two electrodes carrying the waveform.<sup>17,18</sup> A dc “compensation voltage”, also expressed as the compensation field ( $E_C$ ), is superposed on the waveform; scanning  $E_C$  generates the FAIMS spectrum. The resolving power ( $R$ ) strongly depends on the gap shape and gas composition; planar-gap geometries (with a homogeneous field) using He/N<sub>2</sub> or H<sub>2</sub>/N<sub>2</sub> mixtures allow  $R$  up to ~300 for multiply-charged peptides.<sup>19,20</sup> This broadly suffices for baseline separation of variant phosphopeptides in the “bottom-up” size range (1.6 – 1.8 kDa),<sup>14,15</sup> including those alternatively modified on adjacent residues. Proceeding to smaller PTMs and longer “middle-down” sequences (~3 kDa), we have fully resolved<sup>16</sup> all four monoacetylated H4 histone tail variants known *in vivo*, where the PTM mass relative to the peptide mass ( $m_{rel}$ ) is only 1.3%. An obvious question is how far this approach extends to yet smaller PTMs and larger peptides.

The smallest additive PTM is the methyl group (14 Da) that can attach to a lysine or arginine once, twice, or thrice. Here we demonstrate that FAIMS can effectively resolve localization variants of singly and doubly methylated histone tails, where the shifting PTM(s) amount(s) to <1% of the peptide mass.

## Experimental Methods

The custom FAIMS device coupled to an ion trap mass spectrometer via an electrodynamic funnel interface, and parameters of operation utilizing He/N<sub>2</sub> and H<sub>2</sub>/N<sub>2</sub> mixtures have been described.<sup>16</sup> The carrier gas inflow was 2 L/min, leading to the filtering time of ~0.2 s. Samples were dissolved to ~2 – 4  $\mu$ M in 50/49/1 methanol/water/acetic acid and infused to the electrospray source at 0.4  $\mu$ L/min. We have studied human H3 tails purchased from Anaspec (Fremont, CA): (i) the 1 – 21 segment (ARTK<sup>4</sup>QTARK<sup>9</sup>STGGKAPRKQLA) monomethylated on K4 or K9 and (ii) the 21 – 44 segment (ATKAARK<sup>27</sup>SAPATGGVK<sup>36</sup>KPHRYRPG) bismethylated on K27 or K36. These feature C-terminal linkers GG (i) or G (ii) followed by a biotinylated lysine, for total masses of 2737 Da (i) and 2945 Da (ii), with  $m_{rel}$  of 0.51% (i) and 0.95% (ii). Under present conditions, these species create prominent protonated ions with  $z = 5$  and 6 (i) and 4 – 6 (ii). Again, we have used an internal calibrant (the peptide Syntide 2 that produces abundant 2+, 3+, and 4+ ions) and confirmed separations by analyses of 1:1 isomeric mixtures.<sup>14–16</sup>

## Results

We started from the doubly methylated pair (ii). As usual,<sup>14–16</sup> adding He to the gas raises the resolving power as the absolute  $E_C$  increase while the peaks narrow (Figure 1 and Figure S1 in the Supporting Information). The spectral profiles also evolve. Some changes, such as the peak **c/d** for K36 5+ splitting into **c**, **d1**, and **d2**, are attributable to improved resolution, whereas progressive disappearance of higher- $E_C$  features **d** for K36 4+ and **f** for K27 6+ indicates unfolding of more compact conformers induced by field heating in the FAIMS unit.<sup>21</sup> The two variants are best separated using  $z = 5$  at 20 – 40% He, with baseline resolution for the major peaks **b**. Excellent separation of either variant at the dominant peak apexes (**a** for K27 and **b** for K36) is also achieved for  $z = 4$  at 30 – 40% He, whereas K36 can be filtered using **d** at 0 – 20% He. For  $z = 6$ , one can resolve K27 from K36 almost completely (using the major feature **c** at 30 – 40% He), but not vice versa.

As for the acetylated tails,<sup>16</sup> the spectra at 50% H<sub>2</sub> (Figure 1) closely match those at 40% He. Such similarity of conformer distributions using H<sub>2</sub>/N<sub>2</sub> and He/N<sub>2</sub> with greater N<sub>2</sub> fraction is likely due to weaker field heating in H<sub>2</sub>/N<sub>2</sub> than in He/N<sub>2</sub> with equal N<sub>2</sub> amount.<sup>20</sup> The peaks are narrower at 50% H<sub>2</sub> than at 40% He: the mean widths of well-shaped major features are  $\langle w \rangle = 1.5$  V/cm vs. 1.7 V/cm for  $z = 4$  and 1.1 V/cm vs. 1.4 V/cm for  $z = 5 - 6$ . This follows from both lower N<sub>2</sub> content in the H<sub>2</sub>/N<sub>2</sub> mixture and slightly narrower peaks in H<sub>2</sub>/N<sub>2</sub> compared to He/N<sub>2</sub> with same content.<sup>20</sup> With the H<sub>2</sub> concentration going to 70%, the  $E_C$  values increase further while  $\langle w \rangle$  drops to 1.1 V/cm for  $z = 4$  and 0.9 V/cm for  $z = 5 - 6$  (Figure 1 and Figure S2). Higher- $E_C$  features continue to vanish, as seen for K36 4+, K27 6+, and K36 6+. The improved resolving power and peak shifts permit full separation of K27 and K36 for  $z = 6$  at 60% H<sub>2</sub>. However, as the ion signals tend to decrease at higher He or H<sub>2</sub> fractions, the lowest fractions providing sufficient resolution are typically optimum.

The case of single methylation (i) was expected to be more difficult in view of the smaller relative PTM mass and size.<sup>16</sup> Instead, either variants was easily filtered already in N<sub>2</sub>: K4 using a major feature **a** for  $z = 5$  and K9 at the apex of dominant peak **b** for  $z = 6$  (Figure 2). The trends upon He addition track those for bismethylated variants above:  $E_C$  values increase while the peaks narrow and split (Figure S3). Again, some higher- $E_C$  features progressively decrease and vanish, as seen in the transition from **c** to **b** to **a** for K4 5+. However, others (**d2** for K9 5+, **c1** for K4 6+, and **c** for K9 6+) grow at higher He fractions. This perhaps reflects the annealing of metastable unfolded conformers derived from ESI into lower-energy more compact structures.<sup>16</sup> The shift of K9 6+ spectrum to lower  $E_C$  relative to K4 6+ prevents proper filtering of K9 at ~20 – 40% He. The overall resolution still improves at the highest He content, where both variants can be filtered to >96% purity using the major peaks for  $z = 5$  (**a2** for K4 and **d2** for K9) or  $z = 6$  (**c1** for K4 or **b1** for K9). The spectra at 50% and 60% H<sub>2</sub> (Figure S4) resemble those at 40% and 47% He, respectively, but that at 70% H<sub>2</sub> exhibits narrower peaks ( $\langle w \rangle = 1.0$  V/cm) and cleaner variant separation, with K4 **c1** baseline-resolved from K9 **b1** for  $z = 6$  (Figure 2).

Separations of K4 and K9 in various He/N<sub>2</sub> and H<sub>2</sub>/N<sub>2</sub> buffers were verified by analyses of binary mixtures (Figure S5 and Figure 3). A crucial aspect of FAIMS for peptides or other flexible ions is “self-cleaning” – the removal of species that have isomerized and substantially changed  $E_C$  inside the gap.<sup>18,22</sup> This phenomenon, analogous to the elimination of both precursors and products for metastable ions dissociating inside a quadrupole MS filter, may drastically reduce the relative signal for more conformationally flexible peptides. For  $z = 5$ , the rapid attenuation of relative signal for K4 upon He addition likely results from that process promoted by augmented field heating, while K9 (with a much more conserved spectral profile) is affected less. The profiles of both variants depend less on the gas composition for  $z = 6$ , and their relative intensities remain close to the 1:1 molar ratio in solution. These observations illustrate how the intricate distinctions in thermal stability and unfolding pathways of isomeric peptides can affect and assist FAIMS separations.

As the peak capacity of FAIMS for peptides is determined mainly by the relative separation width  $w_{\text{rel}}$  (the ratio of highest to lowest  $E_C$  for different species in a spectrum), the relationship between  $w_{\text{rel}}$  and  $m_{\text{rel}}$  is key to the utility of approach for larger polypeptides. For the previously investigated four-variant sets,  $w_{\text{rel}}$  at the highest He content (in the charge state with maximum  $w_{\text{rel}}$ ) were  $\sim 9m_{\text{rel}}$ , namely  $\sim 0.4$  for phosphopeptides ( $m_{\text{rel}} = 5.0\%$ ) and  $\sim 0.13$  for acetylated peptides ( $m_{\text{rel}} = 1.3\%$ ).<sup>16</sup> Thus,  $w_{\text{rel}}$  would have been  $\sim 0.09$  for present bismethylated and  $\sim 0.05$  for monomethylated peptides. The actual values ( $\sim 0.25$  and  $\sim 0.27$ , respectively) are  $\sim 3 - 5$  times higher already with two species, showing that the variant separation can much exceed the projections from the data for larger PTMs, assuming

proportionality to  $m_{rel}$ . This brightens the prospects for separation of localization variants for yet larger peptides and intact proteins.<sup>16</sup>

## Conclusions

Regioisomers of peptides differing in the site of single or double methylation are readily resolved by FAIMS, even for larger (~3 kDa) peptides where the methyl makes a mere 0.5% of the mass. Along with broad separation of acetylated variants,<sup>16</sup> this enables a new approach to characterization of histones that exhibit extremely complex complements of biologically consequential PTM localizations. Why has FAIMS been immediately able to separate localization variants with all PTMs tried so far, even those minute relative to the whole peptide? An intriguing supposition is that IMS methods exploit the crucial life function of PTMs - adjusting the protein conformations and evolution thereof under external stimuli.

## Supplementary Material

Refer to Web version on PubMed Central for supplementary material.

## Acknowledgments

We thank Ron Moore for experimental help. Parts of this research were supported by NIGMS (GM 067193-09 and GM 103493-10), NCI (CA 155252), Northwestern University Physical Sciences Oncology Center (CA 143869), and the Chicago Biomedical Consortium. Work was performed in the Environmental Molecular Sciences Laboratory, a US DoE national scientific user facility at PNNL.

## References

1. Carey, N. *The Epigenetics Revolution*. Columbia University Press; 2012.
2. Mosmamarast N, Shi Y. *Annu. Rev. Biochem.* 2010; 79:155–179. [PubMed: 20373914]
3. Mann M, Jensen ON. *Nature Biotechnol.* 2003; 21:255–261. [PubMed: 12610572]
4. Sweet SMM, Mardakheh FK, Ryan KJP, Langton AJ, Heath JK, Cooper HJ. *Anal. Chem.* 2008; 80:6650–6657. [PubMed: 18683950]
5. Bailey DJ, Rose CM, McAlister GC, Brumbaugh J, Yu P, Wenger CD, Westphall MS, Thomson JA, Coon JJ. *Proc. Nat'l Acad. Sci.* 2012
6. Kim MS, Pandey A. *Proteomics.* 2012; 12:530–542. [PubMed: 22246976]
7. Molina H, Horn DM, Tang N, Mathivanan S, Pandey A. *Proc. Natl. Acad. Sci. U.S.A.* 2007; 104:2199–2204. [PubMed: 17287340]
8. Sohn CH, Chung CK, Yin S, Ramachandran P, Loo JA, Beauchamp JL. *J. Am. Chem. Soc.* 2009; 131:5444–5459. [PubMed: 19331417]
9. Xuan Y, Creese AJ, Horner JA, Cooper HJ. *Rapid Commun. Mass Spectrom.* 2009; 23:1963–1969. [PubMed: 19504484]
10. Singer D, Kuhlmann J, Muschket M, Hoffman R. *Anal. Chem.* 2010; 82:6409–6414. [PubMed: 20593796]
11. Lindner H, Sarg B, Meraner C, Helliger W. *J. Chromatogr. A.* 1996; 743:137–144. [PubMed: 8817877]
12. Garcia BA, Pesavento JJ, Mizzen CA, Kelleher NL. *Nat. Methods.* 2007; 4:487–489. [PubMed: 17529979]
13. Ibrahim Y, Shvartsburg AA, Smith RD, Belov ME. *Anal. Chem.* 2011; 83:5617–5623. [PubMed: 21692493]
14. Shvartsburg AA, Creese AJ, Smith RD, Cooper HJ. *Anal. Chem.* 2010; 82:8327–8334. [PubMed: 20843012]
15. Shvartsburg AA, Singer D, Smith RD, Hoffmann R. *Anal. Chem.* 2011; 83:5078–5085. [PubMed: 21667994]

16. Shvartsburg AA, Zheng Y, Smith RD, Kelleher NL. *Anal. Chem.* 2012; 84:4271–4276. [PubMed: 22559289]
17. Guevremont R. J. *Chromatogr. A.* 2004; 1058:3–19. [PubMed: 15595648]
18. Shvartsburg, AA. *Differential Ion Mobility Spectrometry: Nonlinear Ion Transport and Fundamentals of FAIMS*. Boca Raton: CRC Press; 2008.
19. Shvartsburg AA, Smith RD. *Anal. Chem.* 2011; 83:23–29. [PubMed: 21117630]
20. Shvartsburg AA, Smith RD. *Anal. Chem.* 2011; 83:9159–9166. [PubMed: 22074292]
21. Shvartsburg AA, Prior DC, Tang K, Smith RD. *Anal. Chem.* 2010; 82:7649–7655. [PubMed: 20666414]
22. Shvartsburg AA, Li F, Tang K, Smith RD. *Anal. Chem.* 2007; 79:1523–1528. [PubMed: 17297950]

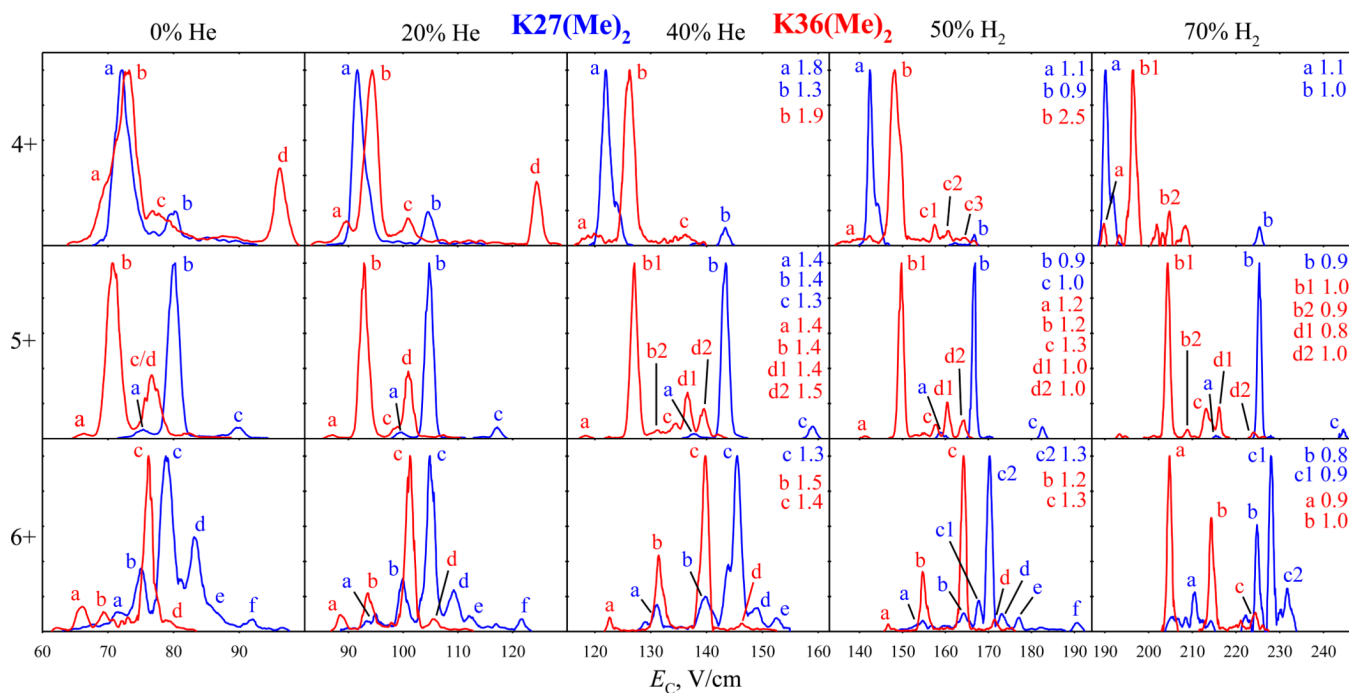


**Fig. 1.** Normalized FAIMS spectra for two bismethylated localization variants of H3 tail (color-coded on the top) with  $z = 4 - 6$ , measured using  $He/N_2$  with 0 – 40% He or  $H_2/N_2$  with 50% or 70%  $H_2$  (v/v), as labeled. Peaks for different conformers are marked by letters. The widths ( $w$ , V/cm) are shown for the well-shaped peaks at 40% He, 50%  $H_2$ , and 70%  $H_2$ . The data for intermediate gas compositions are in Figures S1 and S2.

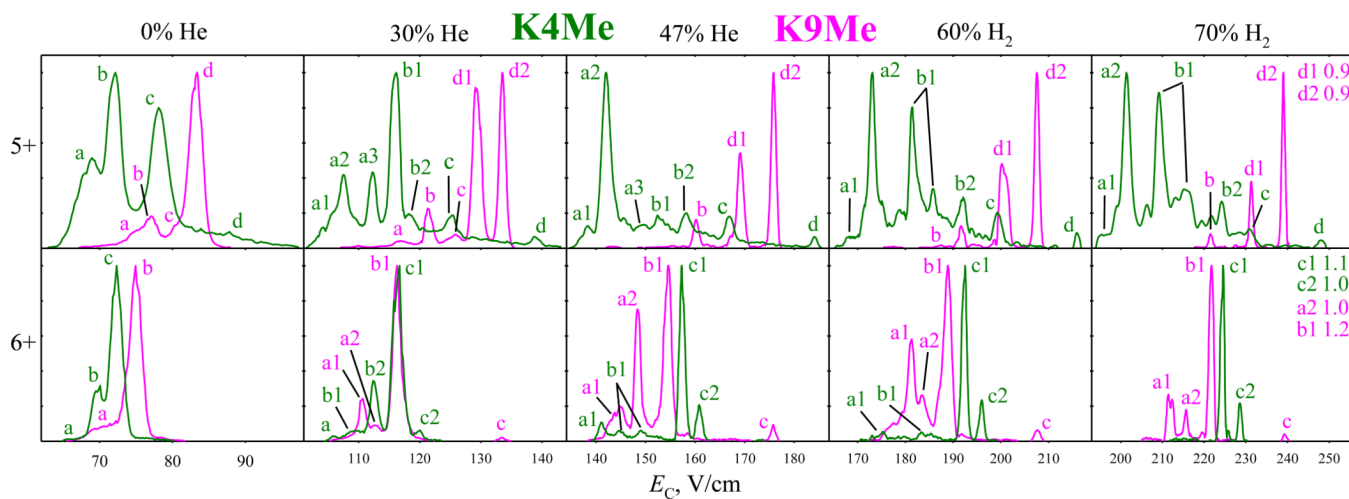


**Fig. 2.** Same as Fig. 1 for two monomethylated variants, measured using He/N<sub>2</sub> with 0 – 47% He or H<sub>2</sub>/N<sub>2</sub> with 60% or 70% H<sub>2</sub>. The data for additional gas compositions are in Figures S3 and S4.

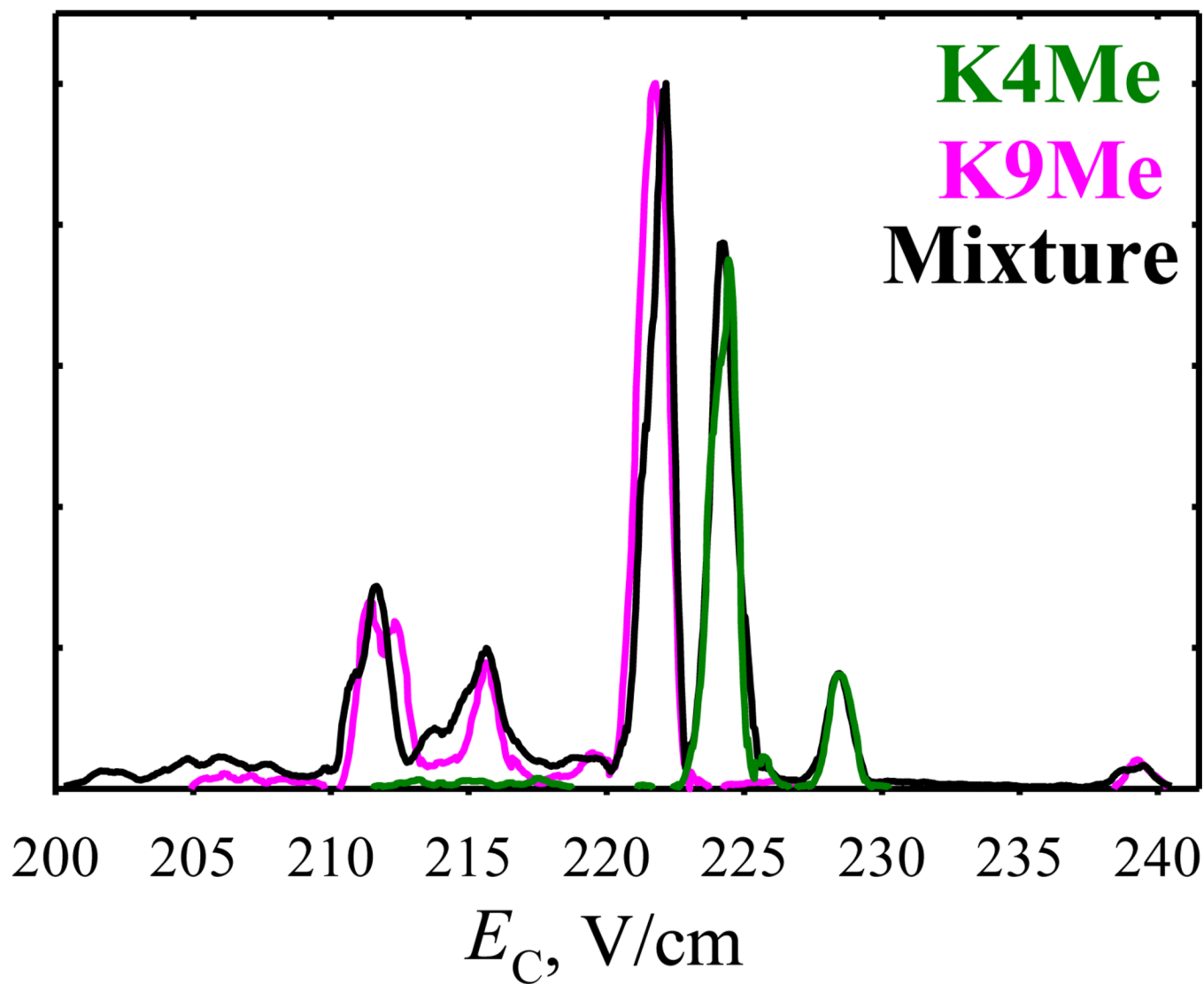


**Fig. 3.**  
FAIMS spectrum for the K4Me/K9Me mixture (6+ ions), measured using 7:3 H<sub>2</sub>/N<sub>2</sub>.  
Vertically scaled spectra for the components are overlaid.